Mine Water and the Environment (2022) 41:704–720
https://doi.org/10.1007/s10230-022-00878-3

TECHNICAL ARTICLE

Geophysical Diagnosis of Diversion Channel Infiltration in a Uranium Waste Rock Pile

Matheus Mistrinel Pacine Feitoza do Nascimento[1] · César Augusto Moreira[1] · Beatriz Guzzo Duz[1] · Ana Júlia Traíba da Silveira[1]

Received: 24 July 2021 / Accepted: 4 May 2022 / Published online: 1 June 2022

Abstract

The Osamu Utsumi mine was the first to economically mine uranium ore in Brazil. During its operation, a river valley was buried for the construction of the waste rock pile. The original stream was diverted to the northwest side of the pile and has since flowed into a diversion channel devoid of basal waterproofing, while an acid mine drainage (AMD) source flows at the base of this waste rock pile. This research aims to evaluate the possible relationship between water infiltration of the diversion channel and the AMD resurgence at the base of the pile using electrical resistivity tomography and induced polarization. 2D inversion models and pseudo-3D maps allowed the recognition of low resistivity zones (< 100 Ω·m) with high chargeability areas (10 mV/V). Some of these low-resistivity areas have been interpreted as infiltration zones in segments of the diversion channel into the pile, and in one of them, the flow intercepts a high chargeability area interpreted as a sulfide-rich zone that is expected to contribute to AMD at the base of the pile. Understanding the hydrogeochemical process will help select effective actions to mitigate the generation of AMD at the mine, which is currently in the decommissioning phase.

Keywords Acid mine drainage · Electrical resistivity tomography · Induced polarization · Uranium mine · Brazil

Introduction

A lack of planning and the failure to observe environmental laws during mine development and operation can negatively affect the physical and biological environment by degrading water courses, soil, and air. (Haddaway et al. 2019; Rubio 2012; Warhate et al. 2006; Younger and Wolkersdorfer 2004). The Brazilian Constitution establishes in Article 225, paragraph 2 "Those who exploit mineral resources shall be required to restore the degraded environment, in accordance with the technical solutions demanded by the competent public agency, as provided by law." (Federative Republic of Brazil 2010). Environmental remediation should occur during mining operations, but they often occur during decommissioning or closure of the mining operations (Castro et al. 2011; Pardo Abad 2019; Smith and Underwood 2000).

Mining can adversely affect water quality by, among other processes, infiltration of mining-influenced water into groundwater and surface water that can lead to contamination of water supplies for cities and agriculture. Acid mine drainage (AMD), in particular, is considered one of the greatest threats to water resources from mining, as it has the potential for devastating long-term impacts to rivers, aquifers, lakes, and aquatic life (Edokpayi et al. 2020; Lghoul et al. 2021; Wolkersdorfer and Bowell 2005).

AMD is generated when sulfide minerals oxidize and interact with water, which causes the conversion of sulfide into sulfate and promotes the formation of sulfuric acid. The acid formed will mobilize chemical elements present in the minerals in the ore, wastes, and country rock, including iron (Fe), aluminum (Al), lead (Pb), and manganese (Mn), forming a low-pH solution with high metal and sulfate concentrations that leach into the environment (Moyé et al. 2017; Nordstrom et al. 2015; Skousen et al. 2018). In the context of uranium (U) mineralization, this factor is aggravated because, in addition to the metals mentioned, U can also be mobilized. Although widely studied, AMD is a complex problem that often requires large investments to mitigate environmental liabilities (Akcil and Koldas 2006).

✉ Matheus Mistrinel Pacine Feitoza do Nascimento
mat_mistrinel@hotmail.com

[1] Geosciences and Exact Sciences Institute (IGCE), São Paulo State University, 24-A Ave, 1515, Bela Vista, Rio Claro, SP, Brazil

The planning of effective measures to reduce environmental impacts caused by AMD requires information about the hydrogeochemical behavior of mine wastes and mined materials, including their mineralogical composition, in addition to the nature for the sulfide oxidation. Some of these can be obtained by geophysical investigations, by measuring physical and electrical parameters associated with the mine wastes, rocks, minerals, and intrapore fluids in an indirect and noninvasive way (Casagrande et al. 2020; Nobes 1996; Targa et al. 2021; Yuval and Oldenburg 1996).

The geophysical methods of electrical resistivity tomography (ERT) and induced polarization (IP) are of great importance in the investigation and study of AMD. ERT allows the identification of high-moisture areas in the subsurface that are usually characterized by low resistivity when compared to drier areas such as unsaturated soils and rocks. AMD has also a geoelectric signature of low resistivity due to a high concentration of dissolved ions that decrease the resistivity of the interstitial fluid. IP allows the identification of sulfide mineralized zones because sulfide mineral surfaces have high chargeability, a physical property related to conductance. Several studies have shown the effectiveness of these geoelectric methods in the identification of AMD and sulfide mineralization zones (Anterrieu et al. 2010; Martín-Crespo et al. 2018; Martínez-Pagán 2021; Moreira et al. 2020; Poisson et al. 2009). Other studies have demonstrated the effectiveness of using ERT to study water infiltration and monitor AMD in waste rock piles (WRP) (Dimech et al. 2019; Greer et al. 2017; Hester et al. 2019; Targa et al. 2019).

Currently, the owner of the Osamu Utsumi Mine, Nuclear Industries of Brazil (INB), is responsible for capturing and treating the acidic mine effluents and ensuring the quality of water from the drainage channels adjacent to the mine. This study attempts to identify water infiltration zones in the WRP and associated with the diversion channel downgradient of the WRP, through the use of ERT and IP geophysical methods.

The Osamu Utsumi Mine

Geological Setting

The study area was the Osamu Utsumi Mine in the municipality of Caldas in the State of Minas Gerais, approximately 10 km from the municipality of Poços de Caldas in southeastern Brazil. It is part of the Poços de Caldas Industrial Mining Complex (CIPC), owned by Nuclear Industries of Brazil (INB), which is a pioneer in the mining and processing of uranium ore in Brazil. The deposit is part of the alkaline complex of Poços de Caldas (CAPC), considered one of the largest occurrences of alkaline rocks in the world and is located in the southern part of the Atlantic Shield near the northeast side of the Paraná Basin (Fraenkel et al. 1985). As detailed in Fig. 1, the CAPC constitutes a circular dome-like

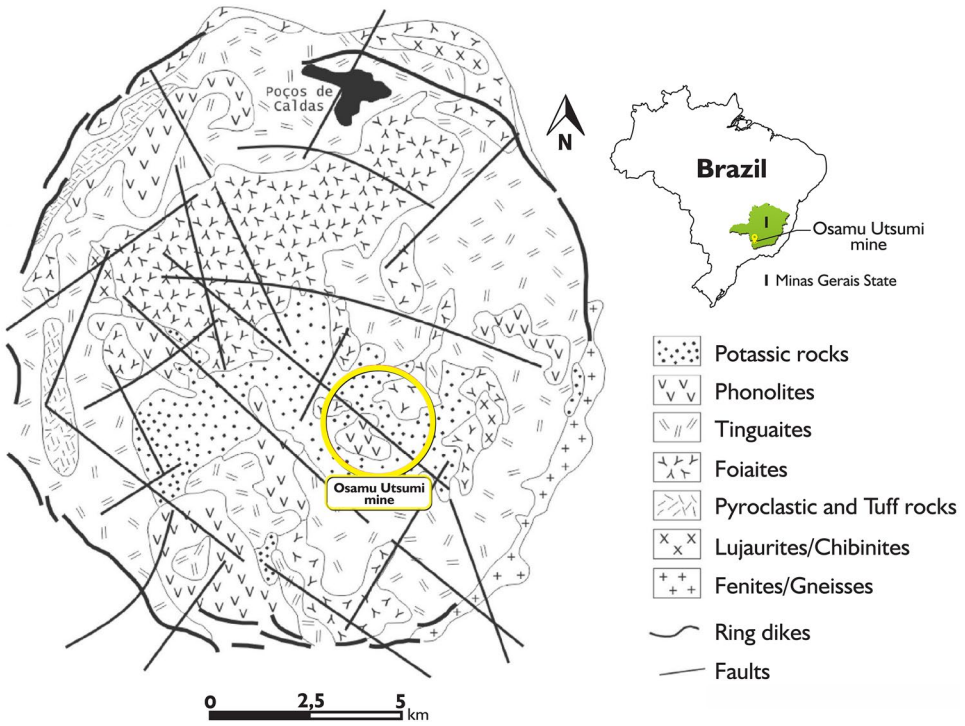

Fig. 1 Geological map of the alkaline complex of Poços de Caldas with emphasis on the location of the Osamu Utsumi Mine (Adapted from Fraenkel et al. 1985).

structure, ≈ 35 km in diameter, marked by ridges and large faults (Costa et al. 2001).

The lithological framework includes effusive (phonolites), hypabyssal (tinguaites), and plutonic alkaline rocks (foiaites), as well as tuff and breccias (Fraenkel 1985). After the intrusion of the foiaites, explosive events occurred that resulted in the formation of a large package of breccias. The permeability of these rocks allowed the percolation of hydrothermal fluids and the formation of U-Th-Zr-F mineralization with rare earth elements (Capovilla 2001; Schorscher and Shea 1992). Hydrothermal alteration was responsible for the argillation and zeolitization of rocks, in addition to pyritization, strong potassium metasomatism, and the formation of radioactive anomalies (Valeton et al. 1997; Waber et al. 1992). The primary minerals associated with the ores are uraninite (UO_2), jordesite (MoS_2), zircon-baddeleyite (ZrO_2), sphalerite (ZnS), fluorite (CaF_2), and pyrite (FeS_2) (Schorscher and Shea 1992).

In the mine area, the lithotypes found include nepheline syenites, tinguaites, phonolites, foiaites, volcanic breccias, and ultrabasic rocks. Multiple igneous events and intense metasomatic and weathering processes resulted in the local lithological assemblage and the formation of disseminated uraninite mineralization (U ore) (Franklin 2007). The main minerals associated with the U ore are pyrite, fluorite, and molybdenum and zircon minerals. There is also a rare type of U ore associated with the zircon and baddeleyite known as caldasite. The discovery of the uraniferous caldasite encouraged the construction of the Osamu Utsumi Mine in 1959 (Cipriani 2002).

Mine Operating History

Currently known as the ore treatment unit (UTM-Caldas), the complex occupies an area of ≈ 15 km^2 and consists of an open pit, ore storage facilities, waste rock piles, the ore processing unit, offices, as well as mine-related treatment impoundments. The mine site includes the boot-out (BF) waste rock piles, with the largest being BF-04 (12.4 million m^3) and BF-08 (14.8 million m^3) piles, which directly resulted from the exploitation of the ore, and the others are from soil stripping (Table 1) (Cipriani 2002).

The ore reserve was calculated at about 17,200 tons of U_3O_8 with a cut-off value of 170 ppm; all material below this value was considered waste and was deposited in the WRP (Cipriani 2002). Daily production reached 2500 tons of ore during operation (Franklin 2007).

The open-pit mining operation consisted of creating 4 m high benches in blocks of 5 m × 5 m × 2 m. The ore was arranged in storage yards for feeding the primary crusher, which reduced rock to fragments 25 cm in size. Then the material passed through secondary crushing and a ball mill that reduced the ore grain size to < 1.168 mm.

In the chemical treatment, the ore was placed in tanks with sulfuric acid at 70 °C for 6 h, with a ratio of 70 to 150 kg H_2SO_4/T of ore. The residue was subjected to a solid–liquid separation process in which it passed through a vacuum mat type filter and was washed with water for maximum U recovery. A clarification process with sodium chlorate was then conducted to remove small mud particles that passed through the filters. Finally, the material was placed in mixing-settling tanks with solvents for the extraction of U, which was subsequently precipitated and concentrated as yellowcake (Cipriani 2002).

This process persisted until 1995 when, due to economic unviability, the Osamu Utsumi Mine was closed. Currently, the mine is in the decommissioning phase, in which it needs to address the environmental liabilities. The AMD occurs mainly in the two largest waste rock piles (BF-04 and BF-08) and is one of the mine's most serious environmental problems.

BF-04 and Consulta Creek Diversion Channel

The research area is located in the northeastern part of the mine site and comprises the interface where the Consulta Creek diversion channel establishes direct contact with the WRP BF-04 (Fig. 2). The BF-04 is ≈ 70 m thick at its greatest depth and occupies an area of ≈ 56.9 ha in the northeastern part of the site. More recent studies indicate an even larger area, of ≈ 65.8 ha and just over 14 million m^3 of waste rocks. BF-04 is divided into two parts. The upper level consists of the overburden resulting from the stripping to reach the ore. The lower level is made of waste rock,

Table 1 Volume, mass, and area estimates of the Osamu Utsumi Mine waste rock piles (Cipriani 2002)

Piles	Volume (1000 m^3)	Mass (1000 T)	Area (ha)	Predominant origin of the material
BF-01	4400	8,800	25.5	Stripping phase
BF-03	9800	19,600	20.5	Stripping phase
BF-04	12,400	24,800	56.9	Stripping phase and screening of ore B
BF-07	2400	4,800	5.3	Stripping phase
BF-08	15,000	30,000	64.4	Stripping phase and screening of ores A and E
BF-CM	560	1,200		Ore E Screening
Total	45,560	89,120	172.6	

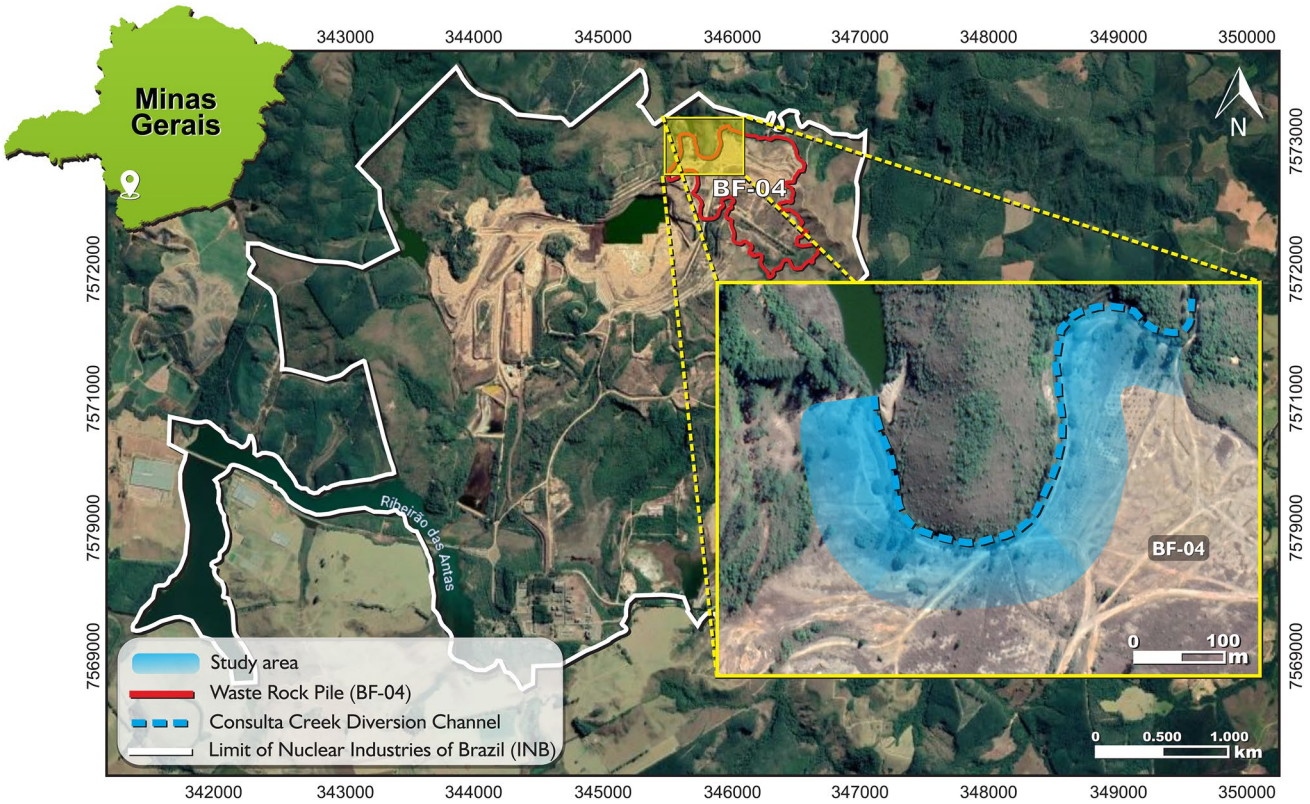

Fig. 2 Location of the study area showing BF-04 and the diversion channel

which contains lower U3O8 concentrations than the cut-off grade of 170 ppm mentioned above (Alberti 2017). This configuration makes the lower level of the BF-04 more prone to AMD generation.

BF-04 was built over the bed of Consulta Creek, in the Rio Verde basin (Fig. 3). BF-04 was constructed by end-dumping; the material was deposited from the top of the pile into the valleys, which resulted in the formation of benches without compaction or drainage control. With this deposition method, the coarser particles are concentrated at the bottom of the slope and the finer particles are concentrated near the crest (Morin et al. 1991; Wilson 2011). A structure formed by end-dumping provides an ideal scenario for the formation of AMD inside the WRP, as it allows water to infiltrate at the top of the pile and oxygen to enter through the coarse particles at the foot of the slope (Pearce et al. 2016).

BF-04's saturated hydraulic conductivity data (K_{sat}) indicate values ranging from 2.06×10^{-4} to 1.04×10^{-3} cm/s for the top of the pile and 9.05×10^{-4} cm/s for the slope at a vertical distance of 5 m below the top. However, the saturated hydraulic conductivity was not measured in the middle or at the foot of the slope due to the presence of coarse- grained material (Franklin 2007). The concentration of coarse material in the lower portion of the end-dumped WRP suggests that the base of the pile has a high hydraulic conductivity, encouraging the discharge of water inside the pile at its base (Franklin 2007). Finally, there is a layer of transition material composed of weathered rock between the WRP and the underlying soil (Franklin 2007).

The average porosity of the BF-04 is 45%, ranging from 35 to 53%, and the average macroporosity values are ≈ 20% higher on the slope than at the top of the pile (Franklin 2007). The high porosity of the WRP and wind currents coming from the valley accelerate the weathering of minerals and contribute to AMD formation (Alberti 2017).

The most abundant minerals identified in the BF-04 waste pile are potassium feldspar [$KAlSi_3O_8$], kaolinite [$Al_2Si_2O_5(OH)_4$], muscovite [$KAl_3Si_3O_{10}(OH)_2$], gibbsite [$Al(OH)_3$], and goethite [FeO(OH)] (Table 2). Sulfide minerals, such as pyrite, are also present at concentrations close to 2%.

Many studies have been carried out on BF-04 since the end of mining activities. Among them, the isopach map showing the thickness of the waste pile, made by Alberti (2017) using digital terrain models (DTM), which were created from a topographic map of the pre-operation period of the mine (1975) and from an aerophotogrammetric survey of the post-operation period of the mine (2010). The isolines present in the isopach map (Fig. 3) correspond to the

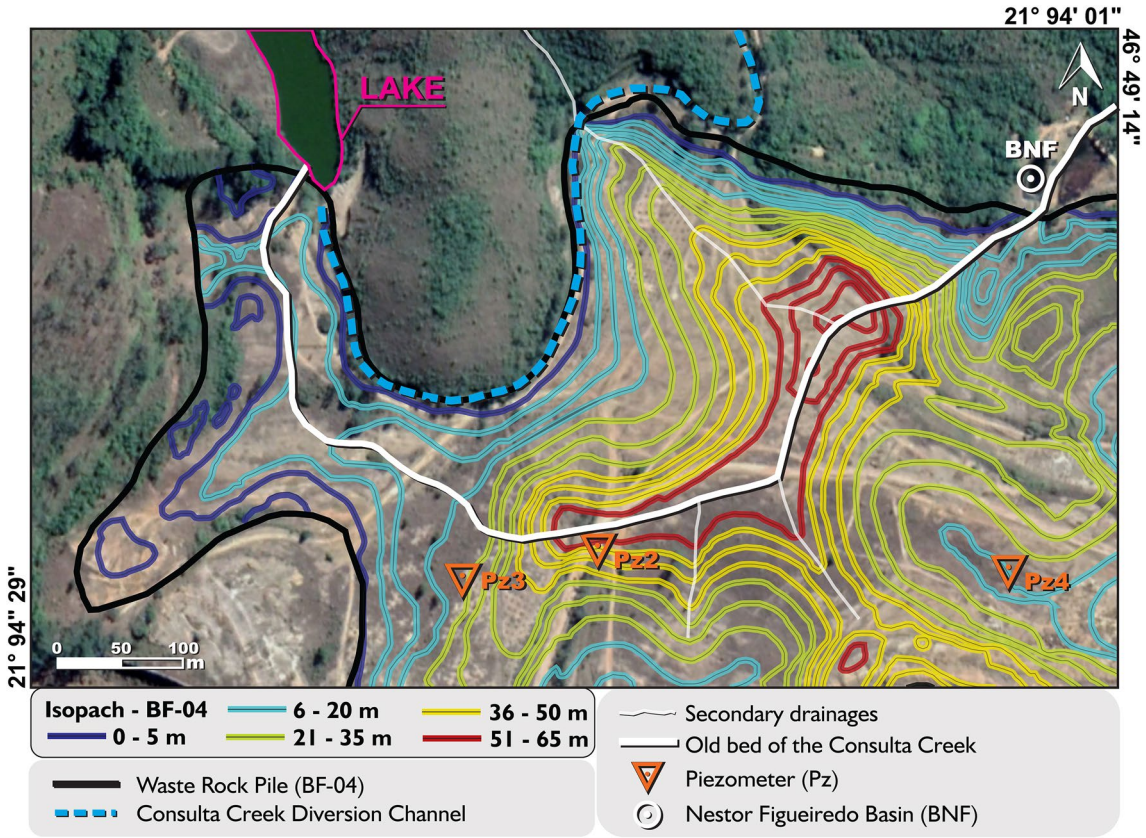

Fig. 3 BF-04 isopach map showing the old bed of Consulta Creek and locations of piezometers Pz2, Pz3 and Pz4. The isolines represent the thickness of the waste rock pile (adapted from Alberti 2017)

Table 2 Mineralogical composition of waste rock in BF-04 according to Franklin (2007) and Leite (2010)

Mineral	Percentages in BF-04 (%)	
	Franklin (2007)	Leite (2010)
K-feldspar ($KAlSi_3O_8$)	50	61.43
Kaolinite ($Al2Si_2O_5(OH)_4$)	20	29.41
Muscovite ($KAl_3Si_3O_{10}(OH)_2$)	20	1.09
Pyrite (FeS_2)	2	–
Barite ($BaSO_4$)	2	–
Goethite (FeO(OH))	2	6.51
Hematite (Fe_2O_3)	1.5	–
Magnetite (Fe_2O_4)	0.5	–
Pyrolusite (MnO_2)	0.17	–
Gibbsite ($Al(OH)_3$)	1.25	1.56
Fluorite (CaF_2)	0.42	–
Uraninite (UO_2)	0.12	–
Silica (SiO_2)	0.4	–

thickness of deposited waste. It is possible to estimate the shape of the topography of the ground below BF-04 since the isopach map indicates the thickness of waste rock and that the surface of BF-04 is predominantly flat. Through the pre-operational DTM of BF-04, it was possible to delineate the bed of Consulta Creek. For better visualization, the old stream bed was superimposed on the BF-04 isopach map (Fig. 3).

Piezometers Pz2 and Pz3 (locations shown in Fig. 3) are both located at an elevation 1376 m and penetrate a waste rock thickness of 51 m and 19.5 m, respectively (Franklin 2007; Table 3). Such thicknesses correspond to those in the isopach map. However, Pz4 has a difference of ≈ 8 m between the value obtained in the piezometer and that in the map. The acid drainage catchment basin (BNF) located at the foot of the BF-04 slope is situated at elevation 1320 m (Fig. 4).

Another interesting factor is the difference between the hydrochemical characteristics at different points in the WRP. The sample from piezometer Pz3 had a low pH (3.5), high SO_4 concentration (22,000 mg/L), and high conductivity (9,850 µS/cm), characteristics that correspond to an environment influenced by AMD. The sample from piezometer Pz4 had a pH of 6.2, 16.4 mg/L of SO_4, and a conductivity of 158 µS/cm. The difference in groundwater quality between piezometers Pz3 and Pz4

Table 3 Average values collected by piezometers from the period 2003 to 2005 and in the BNF from the period 2014 to 2015 concerning water quality in BF-04

	Surface elevation (m)	Waste rock thickness (m)	Transition layer thickness (m)	Ground surface elevation (m)	Ground-water elevation (m)	pH	Spec. Cond. (µS/cm)	SO_4 (mg/L)	References
Pz2	1376	51	6	1319	1327.4	–	–	–	Franklin (2007)
Pz3	1376	19.5	6.5	1351	1356.8	3.5	9853	22,003	
Pz4	1378	24	28	1326	1267	6.2	158	16.4	
BNF	1320	–	–	–	–	4	1297.3	944.3	Alberti (2017)

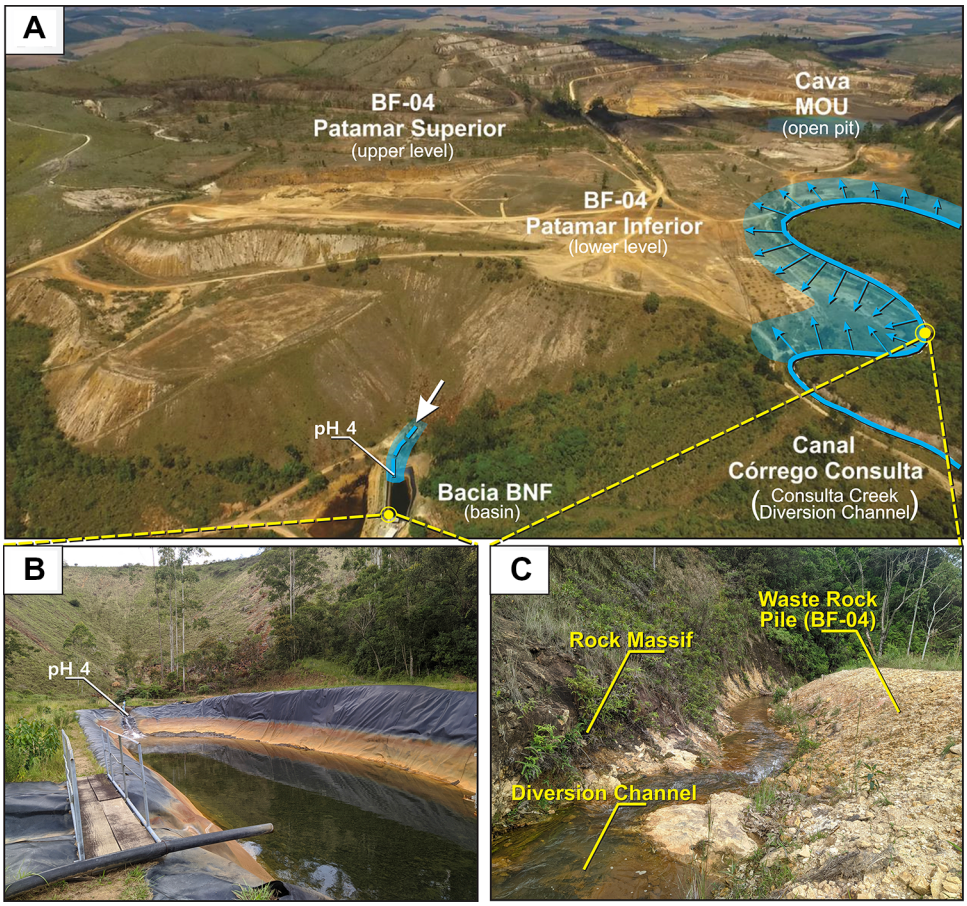

Fig. 4 **A** Aerial view of BF-04 showing the Consulta Creek diversion channel, the possible infiltration zone (blue arrows), and the acid drainage catchment basin (BNF); **B** Acid drainage catchment basin, BNF, at the foot of BF-04; **C** Interaction between the diversion channel, the rocky massif, and the waste rocks pile BF-04

indicates that BF-04 has heterogeneous characteristics, with some areas more susceptible to AMD formation and release than others.

The acid drainage catchment basin (BNF) at the base of BF-04 is designed to collect the effluent generated in the WRP. The historical average flow into the BNF from BF-04 indicates that AMD releases occur both in the rainy and dry months, with the maximum flow in February (72 m^3/h) and the minimum in October (55 m^3/h) (Fagundes 2005). The effluent captured by BNF is characterized by low pH (4), 944 mg/L of SO_4, a conductivity of 1,298 µS/cm and the presence of dissolved constituents such as Si (12.4 mg/L), Al (130 mg/L), Fe (0.86 mg/L), Mn (71.2 mg/L), K (3.50 mg/L), Ca (77.3 mg/L), Mg (7.07 mg/L), and U-nat (140 Bq/L) (Alberti 2017).

At the beginning of mining, the effluent from BF-04 was released directly into Consulta Creek. However, after the problem was identified, the BNF and diversion channel were constructed. Currently, the Consulta Creek diversion channel is 600 m long with an average width of 2 m and is in direct contact with the waste rock pile on one side. The absence of a liner in the channel and its direct connection with BF-04 promotes the transport of AMD from the waste pile and diversion channel to downgradient locations (Fig. 4).

Methods

The geophysical methods applied in the study were ERT and IP. ERT was used to characterize the water flows in porous media and identify acidic and saline conditions in the subsurface related to the generation of AMD. IP was used to recognize zones rich in sulfide minerals (Casagrande 2020; Power 2018). A Schlumberger array, which has a relatively good sensitivity to vertical structures in the subsurface, especially in areas directly below the center of the arrangement, but has relatively poor and limited lateral resolution, was used to measure ERT and IP (Okpoli 2013).

The research campaign lasted two days. Fourteen ERT profiles were conducted for data acquisition along lines that started at the Consulta Creek diversion channel, moved radially into the WRP, and covered the entire area where the diversion channel directly contacts the WRP (Fig. 5). The surface where the profiles were measured is predominantly flat, without significant topographical differences. Lines 1, 2, and 3 had a length of 80 m due to land particularities, and all other lines were 100 m in length, with an electrode spacing of 5 m (17 electrodes for the short profiles and 21 for the long ones); spacing between lines was 45 m.

The electrodes were non-polarizable ceramic and were used as both current and potential electrodes. Each electrode was filled with a copper sulfate solution (Cu-$CuSO_4$), and had a permeable base that allowed for the slow and gradual release of the solution into the soil. In the process of assembling the lines, shallow holes were dug into the soil and filled with water to minimize contact resistance and improve the signal-to-noise ratio.

The equipment used to collect resistivity and chargeability data was an ABEM (Sweden) Terrameter LS resistivity meter. This resistivimeter allows for automatic measurements according to a predefined protocol with a resolution of 1 µV. The unit uses a transmitter power of 250 W, a maximum current of 2.5 A, and allows measurements of DC resistivity, IP, and spontaneous potential (ABEM 2012). Parameters were set for data acquisition as follows: current 1 A, current transmission time of 1 s, start of readings 0.3 s after the current cut-off, and reading of the residual voltage in two consecutive windows of 100 ms each.

The resistivity and chargeability data were processed using the Res2Dinv software package (GEOTOMO SOFTWARE, Malaysia) and produced resistivity/chargeability sections with distance and depth, and a logarithmic graphical scale with interpolation intervals in colors. The software automatically produces a two-dimensional subsurface model from the resistivity or chargeability data obtained from the electrical field measurements (Loke and Baker 1996).

The numerical product of a two-dimensional inversion of data from each section was gathered into a single spreadsheet that combines the position of readings along the lines

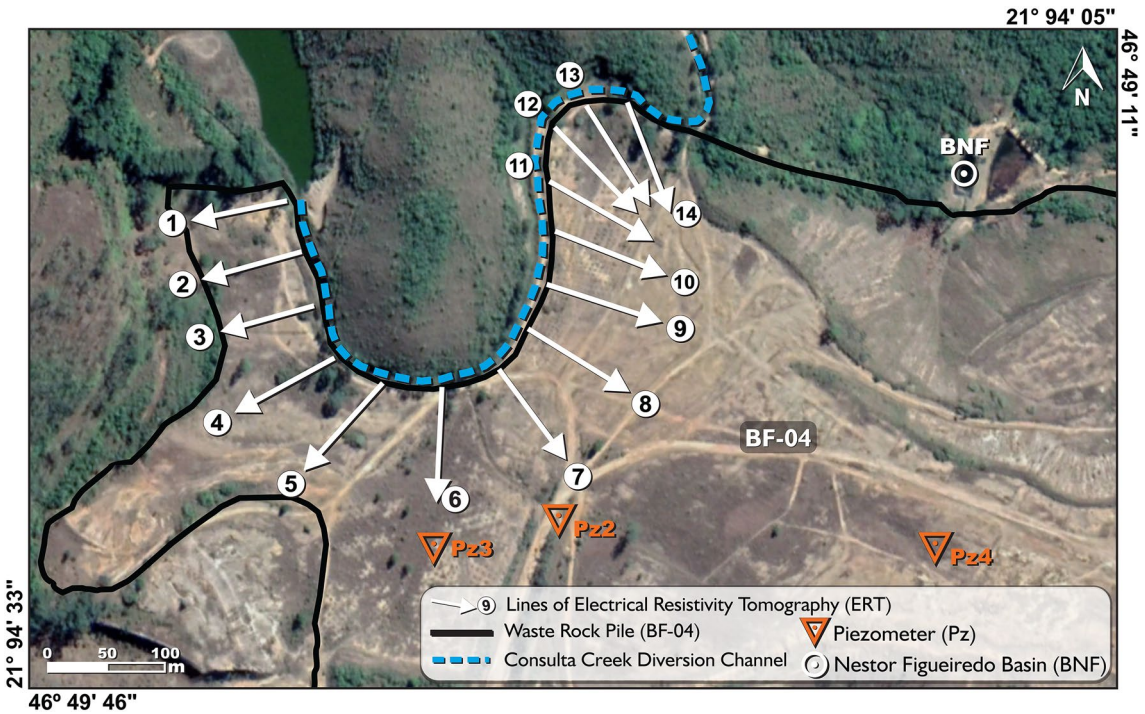

Fig. 5 Geophysical survey lines and locations of the piezometers Pz2, Pz3 and Pz4, the Consulta Creek, and the lake that precedes it

(variable "x"), spacing between lines (variable "y"), depth modeled by the inversion (variable "z"), and the electrical resistivity value (variable "R"). The spreadsheet was used to generate pseudo-3D models, based on a routine of basic steps performed in minerals research. In this case, the sampling plan is often defined from statistics, structural criteria, and spatial placement of a mineral accumulation (Moon et al. 2006).

The 2D model sections were then exported from Res-2dinv to Oasis Montaj Platform (Geosoft) to produce a 3D visualization model for resistivity/chargeability, without topographic data adjustment, also called pseudo-3D or quasi-3D models. 3D visualization models generated from geophysical data are helpful for understanding complex geological structures in mineral exploration and environmental studies (Côrtes et al. 2016; Moreira et al. 2016, 2017a, b; Veloso et al. 2015; Vieira et al. 2016).

Results and Discussion

2D Inversion Models

Data processing and modeling resulted in 14 inversion models for the resistivity parameter and another 14 for chargeability (Figs. 6, 7, 8 and 9). The first three lines reached depths of up to 15.9 m and the others up to 19.8 m, which include the thickness of the WRP at the site and parts of the underlying bedrock.

Some limitations found during the research are noteworthy: the lower resolution at the ends of the ERT lines limited some interpretations; the resolution obtained with the spacing of 5 m between the electrodes does not allow the identification of smaller structures, such as small seepage areas and small volumes of sulfide-rich rocks; and the heterogeneity of the material deposited in BF-04 makes it difficult to identify the boundary between the WRP and the underlying ground surface. Finally, the lack of field-based data, such as stratigraphic information and water levels from piezometers or monitoring wells that crossed any of the ERT lines to support the proposed geophysical model, limited the interpretations. Due to the lack of field-based data, the results of Casagrande (2020), which covered almost the entire lower level of BF-04 using ERT, were used as a reference for the interpretation of resistivity values. In Casagrande's work, the resistivity inversion model number 3 intercepted the previously described piezometer Pz3. The author correlates the water quality data from piezometer Pz3, characterized by low pH (3.5), high SO_4 concentrations (22,003 mg/L), and high conductivity (9853 µS/cm) (Franklin 2007), with a low resistivity zone located near Pz3 in the inversion model. According to the author, the low resistivity would corroborate the low pH and high salinity water in Pz3. Works such as Power et al. (2018) associate anomalies of low resistivity with highly saline water. In the context of BF-04, low resistivity anomalies may represent areas affected by AMD. It is important to highlight the proximity between line 6 presented in this paper and Pz3, which are only 30 m apart.

However, the resistivity values found by Casagrande (2020) ranged from < 10.0 Ω·m to > 12,000 Ω·m, while those found in this work ranged from < 50.0 Ω·m to > 1000 Ω·m. Despite the proximity between some ERT lines, comparison between the two studies is limited due to the difference in resolution between the geophysical models, since the other author used a spacing arrangement of 10 m and reached greater depths.

Different factors are expected to contribute to the saturation and formation of water flow inside BF-04, including rain infiltration, probable infiltration from the diversion channel, and the groundwater associated with the underlying bedrock aquifer. In lines 1, 2, 10, and 12, the shallower zones of low resistivity (< 100 Ω·m) were interpreted as surficial moisture concentration areas, probably resulting from the infiltration of meteoric water (Figs. 6 and 7). In line 1, this moisture is possibly reinforced by the presence of the lake that precedes the diversion channel, located a few meters from the line (Fig. 5). Part of the water within the lake probably infiltrates the northernmost portion of the pile through basement fractures, which are expected to contribute to the potential formation of seepage in the WRP. The maximum thickness of waste rock at the site, indicated by an isopach map (Alberti 2017), could explain the change in resistivity values that occurs close to 10 m in depth. These areas of moderate resistivity (150–540 Ω·m) below 10 m deep were interpreted as a transition layer composed of weathered rocks described by Franklin (2007) (see Table 3).

In lines 1, 2, 6, and 7, there are zones of low resistivity (< 100 Ω·m) located close to the diversion channel interpreted as possible infiltration zones (Fig. 6). It is important to highlight the proximity of these zones to the edge of the inversion models, which can lead to a decrease in the model's resolution in these areas. However, Casagrande (2020) emphasizes that zones of low resistivity with lateral extension toward the diversion channel were identified in most of its sections that are close to the Consulta Creek diversion channel. This fact, according to the author, could indicate possible infiltration of diversion channel waters to the shallower portions of the WRP contributing to the AMD generation process.

The results from lines 7, 8, 9, 10, and 11 show large areas of low resistivity (< 100 Ω·m), interpreted as saturated zones within the WRP close to the old Consulta Creek bed (Figs. 6 and 7). The concave shape of the valley, indicated by the isopach map, possibly contributes to the accumulation of water at the site. The high porosity of the internal part of the WRP and the increase in hydraulic conductivity with

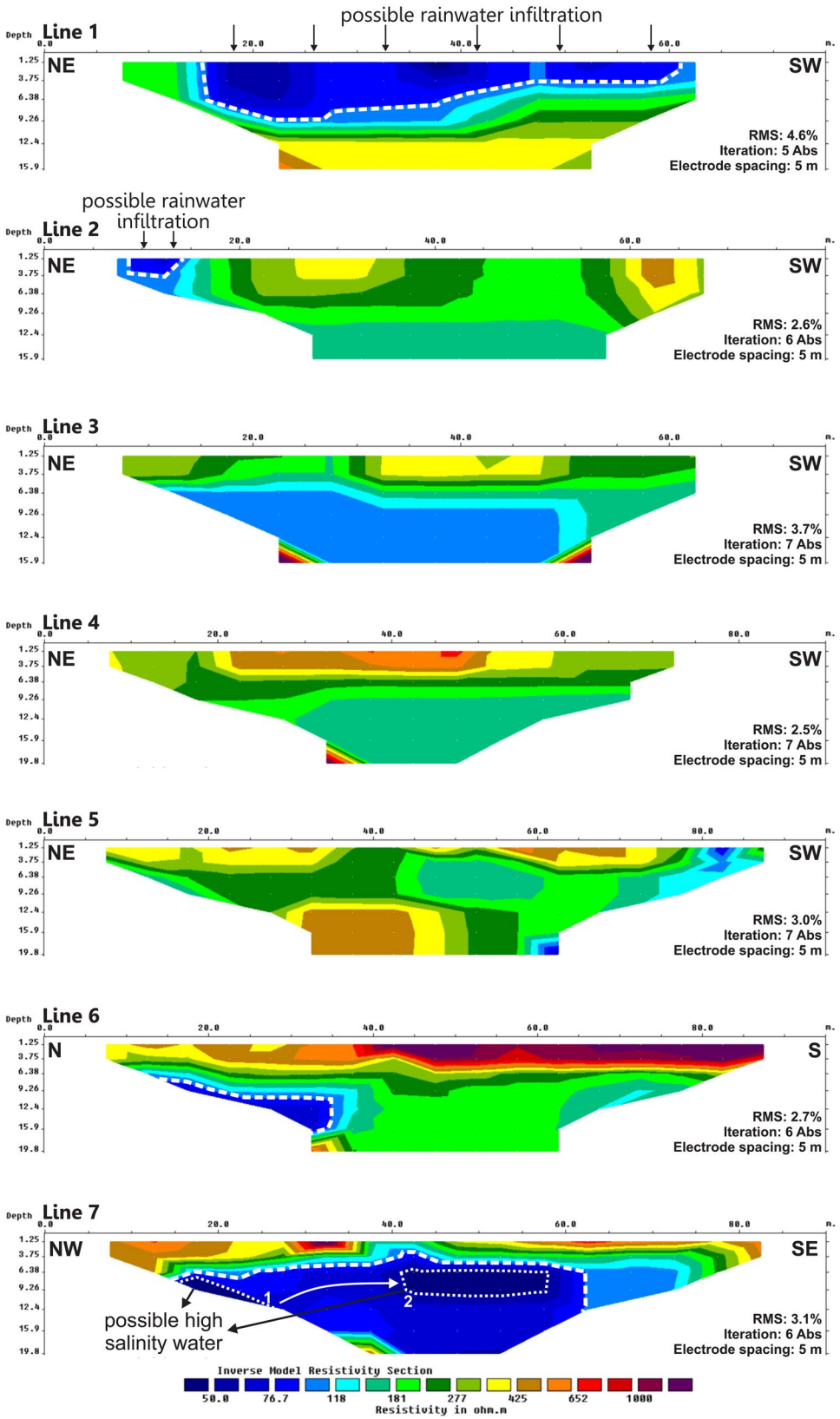

Fig. 6 2D inversion resistivity models for lines 1–7 with possible areas of higher moisture content highlighted. The diversion channel is located to left of all sections. Low resistivity anomalies 1 and 2 are highlighted in line 7

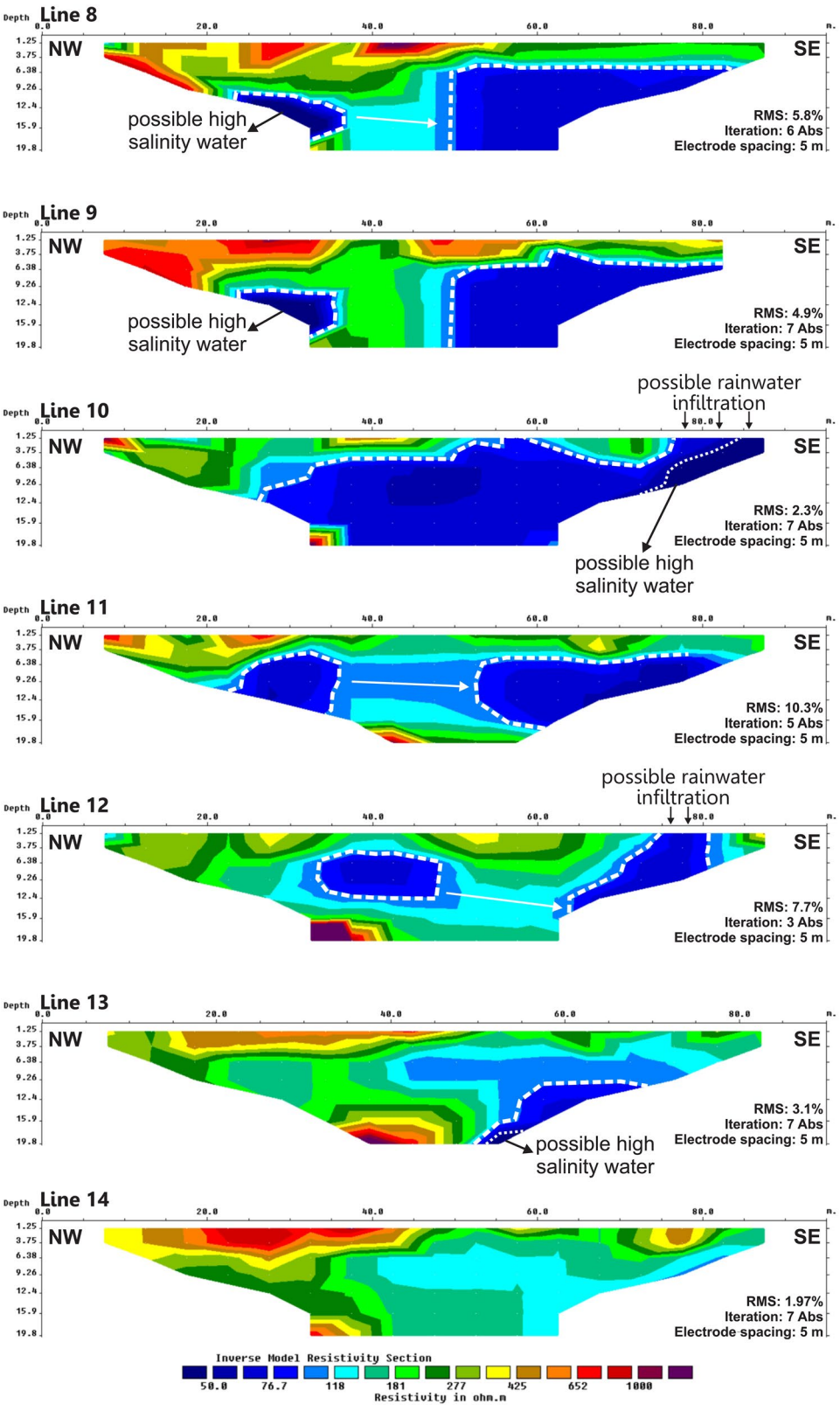

Fig. 7 2D inversion resistivity models for lines 8–14 showing possible areas of higher moisture content. The diversion channel is located to the left on all sections

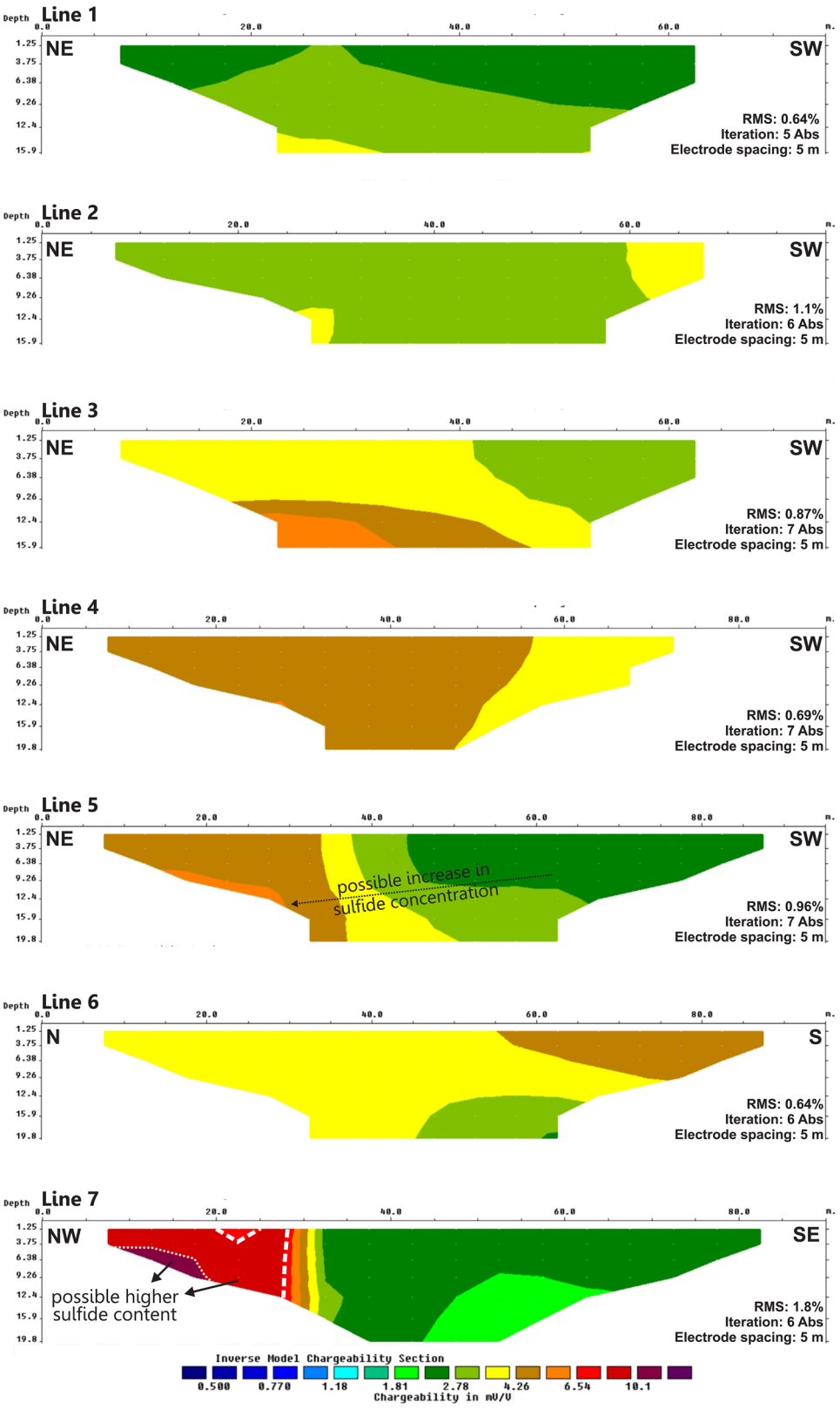

Fig. 8 2D inversion chargeability models for lines 1–7 showing areas of possible higher sulfide content. The diversion channel is located to the left on all sections

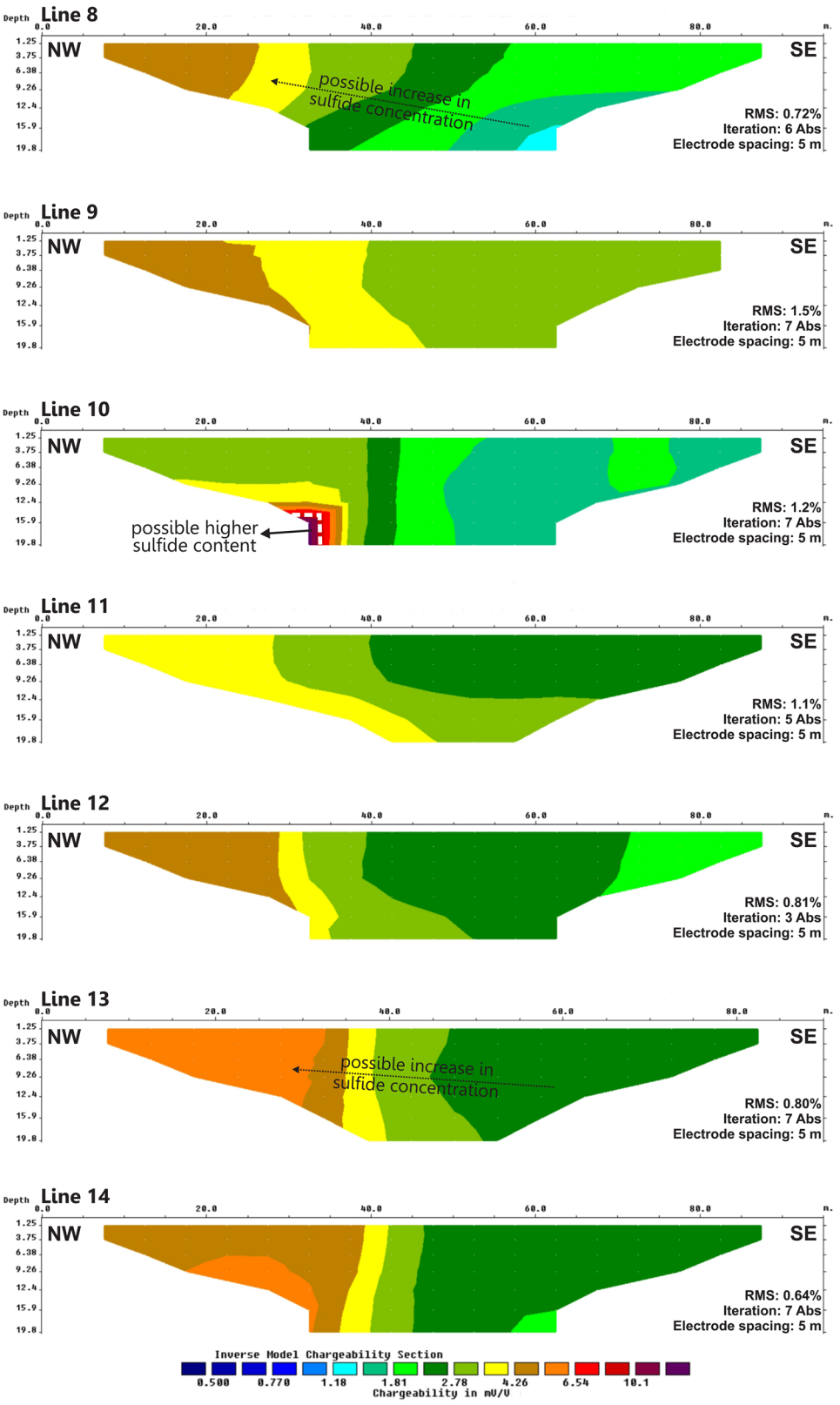

Fig. 9 2D inversion chargeability models for lines 1–7 showing areas of possible higher sulfide content. The diversion channel is located to left of all sections

depth contribute to this hypothesis. The resistivity inversion models 5 and 9 by Casagrande (2020) show an extensive area of low resistivity close to the diversion channel, which reinforces the hypothesis of these areas being saturated.

The low resistivity anomalies (≈ 50 Ω·m) found in lines 7, 8, 9, 10, and 13 were interpreted as possible acidic water areas associated with AMD (Figs. 6 and 7). In line 7, in particular, the model suggests a connection between "anomaly 1" and "anomaly 2." However, it should be noted that the loss of resolution at the ends of sections, where most anomalies occur, can lead to distortions.

Most of the high resistivity zones found in the 2D inversion models were interpreted as unsaturated areas, possibly associated with compacted surface portions of the waste rock pile. The lower porosity and hydraulic conductivity associated with the top of the pile corroborate the hypothesis. Some of the zones of high resistivity also occur at depth, especially in areas close to the diversion channel (Figs. 6 and 7). These were interpreted as portions of the underlying bedrock, as the thickness of the WRP on the left side of the sections of Figs. 6 and 7 are smaller, as evidenced in the isopach map (Fig. 3). Some sections such as 3, 4, 5, and 14 did not show significant moisture concentration zones (Figs. 6 and 7).

The chargeability values were between 0.5 and 10.1 mV/V. Again, the lack of field-based data limited the correlation between chargeability results and possible zones with more abundant disseminated sulfides. Thus, the interpretations made from the chargeability inversion models were based on the chargeability study conducted by Casagrande (2020) that was carried out at the lower level of BF-04. Casagrande (2020) also used the IP method and obtained the same range of chargeability values found in this work.

Studies such as Yuval and Oldenburg (1996) related zones with a sulfide sulfur content close to 4% to chargeability values of 20 mV/V, and areas with low sulfide sulfur percentages (< 1%) with chargeability values between 0.1 to 0.4 mV/V. Many other studies point to a directly proportional relationship between sulfide sulfur content and chargeability (see, e.g. Gurin et al. 2013; Moreira et al. 2016; Rey et al. 2021).

In the context of the study area, the maximum chargeability values (≈ 10.1 mV/V) were interpreted as possible zones of high disseminated sulfide content (Figs. 8 and 9). These zones are possibly associated with portions of the waste rock with higher pyrite content or portions of the underlying rocks that are affected by hydrothermal activity.

The chargeability results in general showed few areas with high values that would indicate the presence of sulfide mineralized zones. The predominance of low chargeability areas is possibly associated with the measured amount of pyrite in the waste rock (≈ 2%) (Franklin 2007). High chargeability zones (≈ 10.1 mV/V) were found in lines 7 and 10, suggesting a higher concentration of sulfides along those lines (Figs. 8 and 9). However, these values need to be interpreted carefully as they are near the ends of the section.

In most sections, there is a tendency for the chargeability values to increase toward the beginning of the lines (0 m) (see Figs. 8 and 9). This trend suggests a higher concentration of sulfides near the diversion channel. The left side in the inversion model of chargeability is characterized by a lower thickness of waste rock due to the steep slope of the underlying ground (Figs. 8 and 9). It is possible that this trend in chargeability values at the site is related to portions of the underlying rocks that have some level of sulfide mineralization.

A possible AMD generation area was found in line 7 (Figs. 6 and 8). The low resistivity anomaly "1" in the section coincides with the high chargeability anomaly near the diversion channel, ≈ 18 m from the origin and ≈ 9 m deep. The zones of low resistivity may also indicate the presence of sulfide mineralization, in addition to humid and high salinity areas. Given this, it is interesting to note that both anomalies occur together. This combination is potentially worrisome since the anomaly of high chargeability indicates a high concentration of sulfides in the site, while the anomaly of low resistivity suggests that the sulfides are present in a saturated porous environment. The combination of high sulfide content alternate wetting and drying contributes to the generation of AMD.

Pseudo-3D Models

From the interpolation of data from the 2D inversion models of resistivity and chargeability, pseudo-3D depth models were created for each physical parameter studied (Fig. 10). The pseudo-3D models presented in this work cover four horizontal levels of visualization at 1 m, 5 m, 9 m, and 13 m deep. From them, it was possible to delineate potential infiltration zones of the Consulta Creek diversion channel into BF-04.

From the resistivity depth slices extracted from the pseudo-3D models (left side of Fig. 10), the observed decrease in resistivity values is interpreted as an increase in humidity or/and an increase in pore water electrical conductivity (EC) with increasing depth. The porosity and hydraulic conductivity of the WRP, which tend to increase with depth, may be related to the increase in areas of low resistivity located in the deeper part of the pseudo-3D resistivity models. The shallower levels show zones of high resistivity that are possibly associated with unsaturated zones in the waste rock or with areas where the waste is more compacted. The least resistive surface areas (< 100 Ω·m) were interpreted as areas of higher moisture content, possibly related to infiltration of meteoric water.

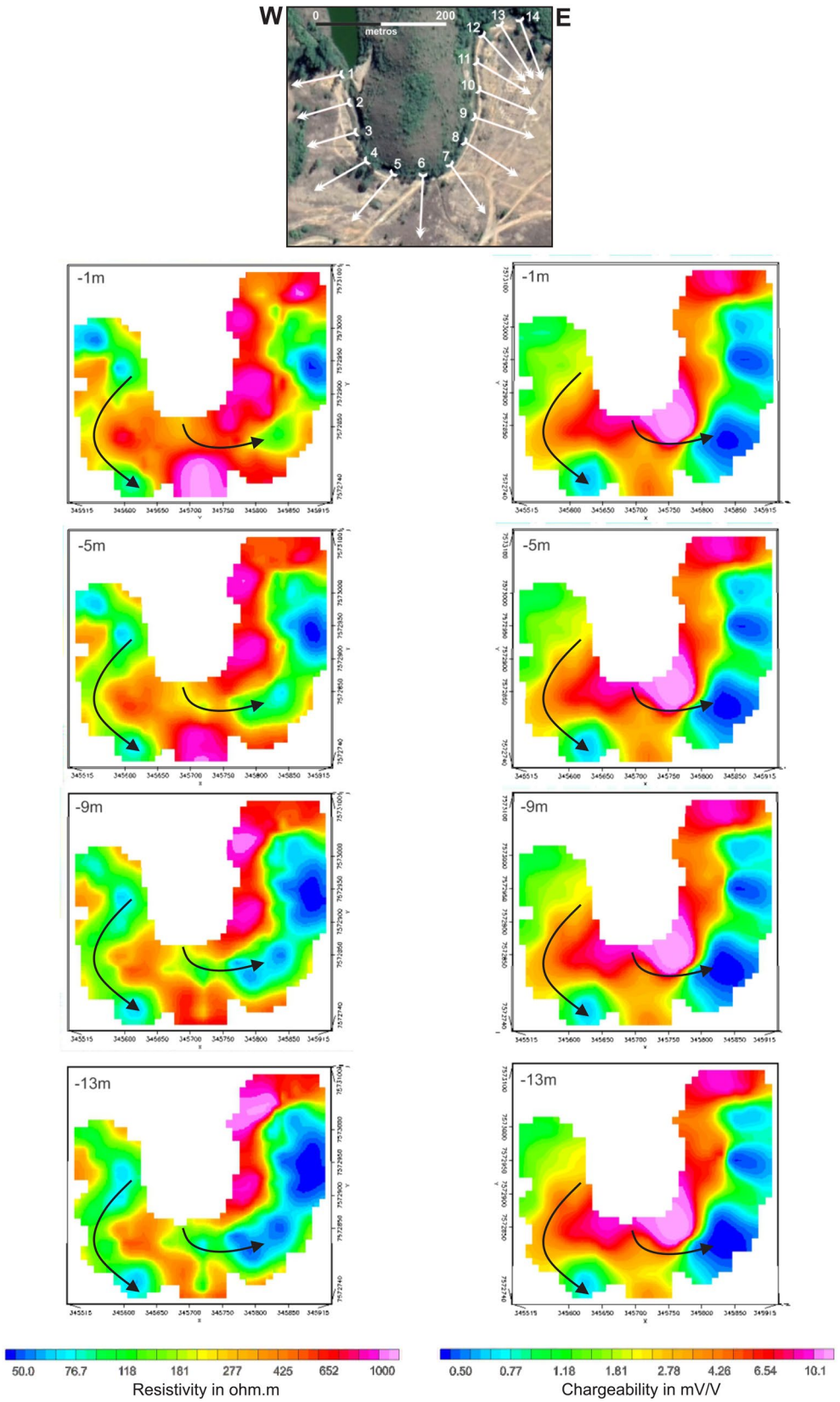

Fig. 10 Pseudo-3D models at 1 m, 5 m, 9 m, and 13 m depth for resistivity and chargeability with proposed hydrogeological flow indicated by black arrows

Two possible zones of infiltration from the Consulta Creek diversion channel into BF-04 were interpreted from the pseudo-3D resistivity models (see Fig. 10). The first one is located in the northwest part, near lines 1 and 2, and is characterized as a low resistivity zone (< 100 Ω·m) possibly connected to the channel. This low resistivity zone was interpreted as an area of higher moisture content associated with the underlying bed of Consulta Creek. Both areas, the low resistivity zone and the stream bed, have a similar shape. Given the proximity to the lake, it is possible that some of the waters retained by the lake infiltrate into BF-04 through the old stream bed and create a preferential flow path that follows the underlying streambed. Another hypothesis would be the infiltration of water from the diversion channel.

The low resistivity zones associated with the first possible infiltration area occur at all four depth levels (see Fig. 10), which suggests that higher moisture content is present both within the WRP and in the transition layer below (see Table 3). The isopach map indicates a maximum thickness of waste rock of 10 m for the site.

The second possible infiltration zone on BF-04 is located near the beginning of line 6, in the central portion of the model. It is characterized by a low resistivity zone identified from 9 m deep. Integrated analysis with the BF-04 isopach map suggests that this low resistivity zone is possibly connected to low resistivity areas located in the eastern portion of the model, possibly forming a preferential flow path. According to the isopach map (see Fig. 3), the site has a steep slope in the underlying ground that dips in the southeast/east direction. Another factor in this possible infiltration zone is the presence of zones of high chargeability (≈ 10.1 mV/V), interpreted as areas with a higher sulfide content, close to zones of low resistivity (< 100 Ω·m), which are interpreted as areas of higher moisture content. In the context of BF-04, the presence of sulfide-rich zones in contact with water could lead to the generation of AMD.

In the eastern portion of the pseudo-3D resistivity and chargeability model graphs (see Fig. 10), there is an extensive area characterized by low resistivity and chargeability values interpreted as a possible zone with higher moisture content zone with probable acidic leachate, suggested by anomalous areas of low resistivity (< 50 Ω·m). The chemical characteristics of BNF leachate (pH 4) contribute to the hypothesis. The moisture content is probably related to the shape of the Consulta Creek streambed, which would control water flow in BF-04. The isopach map and the work by Casagrande (2020) corroborate the hypothesis of water accumulation in this location.

In contrast to the low resistivity and chargeability zones in the eastern portion of the study area, there is a similarly shaped area of moderate to high values below 9 m deep in both models (see Fig. 10). This area was interpreted as the underlying ground surface. This assumption is reinforced in the isopach map (see Fig. 3), which shows a similar configuration in the underlying rock at the site.

Conclusions

The integrated use of (ER) and (IP) methods was considered satisfactory for identifying subsurface structures in the context of BF-04. In the proposed geophysical model, many areas of low resistivity (< 100 Ω·m) were identified and interpreted as zones of higher moisture content. The joint analysis of the resistivity data with the WRP porosity and hydraulic conductivity data suggests the possible occurrence of leachate fluxes within the pile, mainly in the deeper areas.

Some of these flows may be associated with the pre-existing bed of Consulta Creek and are possibly propagated in the transition zone below the WRP. It is probable that the stream, which was buried for the construction of BF-04, acts as a preferential pathway for the existence and movement of moist areas within the pile. This hypothesis is reinforced by the 2D inversion and the pseudo-3D models.

Two possible infiltration zones were identified near the diversion channel. The first one is located on the west side of the channel, near lines 1 and 2, and has a possible relationship with the Consulta Creek streambed. The second probable zone, located near line 6, appears in the 3D-pseudo model from 9 m deep and lower, which suggests that infiltration may occur instead at depth.

Due to the radial positioning of the ERT lines, the diversion channel was located near the one end of the models, where a significant loss of resolution occurs. This fact limited the interpretations. However, the geophysical model proposed also corresponds with the data presented by other authors, including the isopach map of BF-04 and the location of the Consulta Creek streambed, suggesting relative confidence in the geophysical model presented.

The low chargeability values found in the models suggest a low sulfide content in the waste rock, since high chargeability values were interpreted as zones of higher sulfide content. Only two areas of high chargeability were found. In one (line 7) the integrated analysis with the 2D inversion resistivity model indicated the possibility of AMD generation at the site.

The lack of field-based data in the area reinforces the need for additional research at the site. A proposed geophysical model may help identify ideal locations for citing of new monitoring wells and piezometers in BF-04.

Finally, the two possible infiltration zones found in the research would have the potential to directly contribute to increased water availability within BF-04 that could promote AMD generation. Thus, lining of the channel in the places where these possible infiltrations occur could reduce the volume of water flowing into the pile and consequently

reduce the AMD captured by BNF. These changes could reduce AMD treatment costs and minimize environmental effects in the future.

Acknowledgements The authors thank the São Paulo Research Foundation (FAPESP) for funding the project "Sustainable decommissioning: analysis of hydrogeological behaviour in rock massifs and their influence on geotechnical stability in open pit mine slopes and acid mine drainage generation" (2020/14647-0), the Coordination for the Improvement of Higher Education Personnel (CAPES) for financial support, and the INB for collaborating and allowing the fieldwork, with technical support and access to data and the study area.

References

ABEM (2012) Terrameter LS—Instruction manual. ABEM Instrument, Sundbyberg, Sweden

Akcil A, Koldas S (2006) Acid Mine Drainage (AMD): causes, treatment and case studies. J Clean Prod 14:1139–1145. https://doi.org/10.1016/j.jclepro.2004.09.006

Alberti HL (2017) Estudo hidroquímico e isotópico das águas subterrâneas impactadas pela drenagem ácida da mina de urânio—Osamu Utsumi, Planalto de Poços de Caldas (MG). State Univ of Campinas, Thesis ((**in Portuguese**))

Anterrieu O, Chouteau M, Aubertin M (2010) Geophysical characterization of the large-scale internal structure of a waste rock pile from a hard rock mine. Bull Eng Geol Environ 69:533–548. https://doi.org/10.1007/s10064-010-0264-4

Capovilla MNGM (2001) Urânio nos hidrotermalitos potássicos ("rocha potássica") da Mina Osamu Utsumi, Complexo Alcalino de Poços de Caldas. PhD Diss, Univ of São Paulo (in Portuguese), MG

Casagrande MFS, Moreira CA, Targa DA (2020) Study of generation and underground flow of acid mine drainage in waste rock pile in uranium mine using electrical resistivity tomography. Pure Appl Geophys 77:703–721. https://doi.org/10.1007/s00024-019-02351-9

Castro M, Lima H, Flôres J (2011) Overview of mine closure in Minas Gerais. Brazil Revista Escola De Minas 64(2):205–211. https://doi.org/10.1590/s0370-44672011000200012

Cipriani M (2002) Mitigação dos impactos sociais e ambientais decorrentes do fechamento definitivo de minas de urânio. Thesis, State Univ of Campinas (in Portuguese)

Côrtes ARP, Moreira CA, Veloso DIK, Vieira LB, Bergonzoni FA (2016) Geoelectrical prospecting for a coppersulfide mineralization in the Camaquã sedimentary basin, southern Brazil. Geofís Int 55:107–117

Costa PCG (2001) Projeto hidrogeoambiental das estâncias hidrominerais da Companhia Mineradora de Minas Gerais–COMIG – Estância Hidromineral de Poços de Caldas. Technical Report, COMIG/Fundação Gorceix (Portuguese)

Dimech A, Chouteau M, Aubertin M, Bussière B, Martin V, Plante B (2019) Three-dimensional time-lapse geoelectrical monitoring of water infiltration in an experimental mine waste rock pile. Vadose Zone J 18(1):1–19. https://doi.org/10.2136/vzj2018.05.0098

Edokpayi JN, Makungo R, Mathivha F, Rivers N, Volenzo T, Odiyo JO (2020) Influence of global climate change on water resources in South Africa: toward an adaptive management approach. In: Ch 5, Water Conservation and Wastewater Treatment in BRICS Nations, Elsevier, pp 83–115. https://doi.org/10.1016/B978-0-12-818339-7.00005-9

Fagundes JRT (2005) Balanço hídrico do bota-fora BF4 da mina de Urânio Osamu Utsumi, como subsídio para projetos de remediação de drenagem ácida. In: MS Diss, Programa de Pós-Graduação em Engenharia Civil, Escola de Minas, Federal Univ of Ouro Preto, Brazil 59 (in Portuguese)

Federative Republic of Brazil (2010) Constitution of the Federative Republic of Brazil, 3rd Edition. https://www.oas.org/es/sla/ddi/docs/acceso_informacion_base_dc_leyes_pais_b_1_en.pdf

Fraenkel MO, Santos RC, Loureiro FEVL, Muniz WS (1985) Jazidas de urânio no Planalto de Poços de Caldas—Minas Gerais. In: Principais minerais do Brasil, vol 1. MMe, DNPM e CVRD, pp 89–103 (in Portuguese)

Franklin MR (2007) Modelagem numérica do escoamento hidrológico e dos processos geoquímicos aplicados à previsão da drenagem ácida em uma pilha de estéril da mina de urânio de Poços de Caldas—MG. Thesis, Federal Univ of Rio de Janeiro (in Portuguese)

Geotomo software (2003) Geoelectrical imaging 2D & 3D. https://www.geotomosoft.com/downloads.php

Greer BM, Burbey TJ, Zipper CE, Hester ET (2017) Electrical resistivity imaging of hydrologic flow through surface coal mine valley fills with comparison to other landforms. Hydrol Process 31(12):2244–2260. https://doi.org/10.1002/hyp.11180

Gurin G, Tarasov A, Ilyin Y, Titotv K (2013) Time domain spectral induced polarization of disseminated electronic conductor: laboratory data analysis through the Debye decomposition approach. J Appl Geophys 98:44–53. https://doi.org/10.1016/j.jappgeo.2013.07.008

Haddaway NR, Cooke SJ, Lesser P, Macura B, Nilsson AE, Taylor JJ, Raito K (2019) Evidence of the impacts of metal mining and the effectiveness of mining mitigation measures on social–ecological systems in Arctic and boreal regions: a systematic map protocol. Environ Evid 8:9. https://doi.org/10.1186/s13750-019-0152-8

Hester ET, Little KL, Buckwalter JD, Zipper CE, Burbey TJ (2019) Variability of subsurface structure and infiltration hydrology among surface coal mine valley fills. Sci Total Environ 651:2648–2661. https://doi.org/10.1016/j.scitotenv.2018.10.169

Leite JSM (2010) Previsão de drenagem ácida por meio de testes estáticos do material do bota fora 4 da mina Osamu Utsumi –Caldas/MG. Master's diss, Programa de Pós-Graduação em Evolução Crustal e Recursos Naturais, Dept de Geologia, Escola de Minas, Federal Univ of Ouro Preto, Brazil. 59 (in Portuguese)

Lghoul M, Sbihi K, Maqsoud A, Hakkou R, Kchikach A (2021) Remediation scenario of the abandoned Kettara mine site (Morocco): acid mine drainage (AMD) transport modeling. SN Appl Sci 3:702. https://doi.org/10.1007/s42452-021-04690-6

Loke MH, Baker RD (1996) Rapid least squares inversion of apparent resistivity pseudosections by quasi-Newton method. Geophys Prospect 44:131–152. https://doi.org/10.1111/j.1365-2478.1996.tb00142.x

Martín-Crespo T, Gómes-Ortiz D, Marín-Velázquez S, Martínez-Pagán P, Ignacio C, Lillo J, Faz A (2018) Geoenvironmental characterization of unstable abandoned mine waste rocks combining geophysical and geochemical methods (Cartagena-La Union district, Spain). Eng Geol 232:135–146. https://doi.org/10.1016/j.enggeo.2017.11.018

Martínez-Pagán P, Gómez-Ortiz D, Martín-Crespo T, Martín-Velázquez S, Martínez-Segura M (2021) Electrical resistivity imaging applied to waste rocks ponds: an overview. Mine Water Environ. https://doi.org/10.1007/s10230-020-00741-3

Moon CJ, Whateley MEG, Evans AM (2006) Introduction to mineral exploration. Backwell Publishing, Oxford

Moreira CA, Carrara A, Helene LPI, Hansen MAF, Malagutti Filho W, Dourado JC (2017a) Electrical resistivity tomography (ERT) applied in the detection of inorganic contaminants in suspended aquifer in Leme city (Brazil). Rev Brasil De Geofís 35:213–225. https://doi.org/10.22564/rbgf.v35i3.848

Moreira CA, Helene LPI, Côrtes ARP (2017b) DC resistivity method applied in the monitoring of diesel leakage in a railway accident

in São Manuel city, São Paulo State (Brazil). Rev Brasil De Geofís 35:5–14. https://doi.org/10.22564/rbgf.v35i1.969
Moreira CA, Casagrande MFS, Büchi FMS, Targa DA (2020) Hydrogeological characterization of a waste rock pile and bedrock affected by acid mine drainage from geophysical survey. SN Appl Sci 2:1236. https://doi.org/10.1007/s42452-020-3021-8
Moreira CA, Lapola MM, Carrara A (2016) Comparative analyzes among electrical resistivity tomography arrays in the characterization of flow structure in free aquifer. Geofís Int, 55(2):119–129. http://revistagi.geofisica.unam.mx/index.php/RGI/article/view/1716/1592
Morin KA, Gerencher E, Jones CE, Konasewich DE (1991) Critical literature review of acid drainage from waste rock. MEND Rep 1(11):1
Moyé J, Picard-Lesteven T, Zouhri L, Amari KE, Hibti M, Benkaddour A (2017) Groundwater assessment and environmental impact in the abandoned mine of Kettara (Morocco). Environ Pollut 231:899–907. https://doi.org/10.1016/j.envpol.2017.07.044
Nobes DC (1996) Troubled waters: environmental applications of electrical and electromagnetic methods. Surv Geophys 17:393–454. https://doi.org/10.1007/BF01901640
Nordstrom DK, Blowes DW, Ptacek CJ (2015) Hydrogeochemistry and microbiology of mine drainage: an update. Appl Geochem 57:3–16. https://doi.org/10.1016/j.apgeochem.2015.02.008
Okpoli CC (2013) Sensitivity and resolution capacity of electrode configurations. Int J Geophys. https://doi.org/10.1155/2013/608037
Pardo Abad CJ (2019) Environmental recovery of abandoned mining areas in Spain: sustainability and new landscapes in some case studies. J Sustain Res 1:e190003. https://doi.org/10.20900/jsr20190003
Pearce S, Lehane S, Pearce J (2016) Waste material placement options during construction and closure risk reduction—quantifying the how, the why and the how much. In: AB Fourie & M Tibbett (eds). Mine Closure, Australian Centre for Geomechanics. https://doi.org/10.36487/ACG_rep/1608_51_Pearce
Poisson J, Chouteau M, Aubertin M, Campos D (2009) Geophysical experiments to image the shallow internal structure and the moisture distribution of a mine waste rock pile. J Appl Geophys 67:179–192. https://doi.org/10.1016/j.jappgeo.2008.10.011
Power C, Tsourlos P, Ramasamy M, Nivorlis A, Mkandawire M (2018) Combined DC resistivity and induced polarization (DC-IP) for mapping the internal composition of a mine waste rock pile in Nova Scotia, Canada. J Appl Geophys 150:40–51. https://doi.org/10.1016/j.jappgeo.2018.01.009
Rey J, Martínez J, Hidalgo MC, Mendoza R, Sandoval S (2021) Assessment of tailings ponds by a combination of electrical (ERT and IP) and hydrochemical techniques (Linares, southern Spain). Mine Water Environ. https://doi.org/10.1007/s10230-020-00709-3
Rubio RF (2012) Mining: the challenge knocks on our door. Mine Water Environ 31:69–73. https://doi.org/10.1007/s10230-012-0169-5
Schorscher HD, Shea ME (1992) The regional geology of the Poços de Caldas alkaline complex: mineralogy and geochemistry of selected nepheline syenites and phonolites. J Geochem Explor 45:25–51. https://doi.org/10.1016/0375-6742(92)90121-N
Skousen JG, Ziemkiewicz PF, McDonald LM (2018) Acid mine drainage formation, control and treatment: approaches and strategies. Extractive Ind Soc 6(1):241–249. https://doi.org/10.1016/j.exis.2018.09.008
Smith FW, Underwood B (2000) Mine closure: the environmental challenge. Min Technol 109(3):202–209. https://doi.org/10.1179/mnt.2000.109.3.202
Targa DA, Moreira CA, Camarero PL, Casagrande MFC, Alberti HLC (2019) Structural analysis and geophysical survey for hydrogeological diagnosis in uranium mine, Poços de Caldas (Brazil). SN Appl Sci 1:299. https://doi.org/10.1007/s42452-019-0309-7
Targa DA, Moreira CA, Casagrande MFS (2021) Hydrogeological analysis of sulfide waste rocks at a uranium mine using geophysical and hydrochemical methods. Mine Water Environ. https://doi.org/10.1007/s10230-021-00791-1
Valeton I, Schumann A, Vinx R, Wieneke M (1997) Supergene alteration since the upper cretaceous on alkaline igneous and metasomatic rocks of the Poços de Caldas ring complex, Minas Gerais, Brazil. Appl Geochem 12:133–154. https://doi.org/10.1016/S0883-2927(96)00060-1
Veloso DIK, Moreira CA, Côrtes ARP (2015) Integration of geoelectrical methods in the diagnostic of a diesel contaminated site in Santa Ernestina (SP, Brazil). Rev Brasil De Geofís 33(4):667–676. https://doi.org/10.22564/rbgf.v33i4.760
Vieira LB, Moreira CA, Côrtes ARP, Luvizotto GL (2016) Geophysical modeling of the manganese deposit for induced polarization method in Itapira (Brazil). Geofís In 55:107–117. http://revistagi.geofisica.unam.mx/index.php/RGI/article/view/1715/1591
Waber N, Schorscher HD, Tj P (1992) Hydrothermal and supergene uranium mineralization at the Osamu Utsumi mine, Poços de Ca1das, Minas Gerais, Brazil. J Geochem Explor 45:53–112. https://doi.org/10.1016/0375-6742(92)90122-O
Warhate SR, Yenkie MKN, Chaudhari MD, Pokale WK (2006) Impacts of mining activities on water and soil. J Environ Sci Eng 48(2):81–90
Wilson GW (2011) Rock dump hydrology: an overview of full-scale excavations and scale-up experiments conducted during the last two decades. In: Bell LC, Braddock B (Eds), Proc, 7th Australian Workshop on Acid and Metalliferous Drainage, pp 307–322
Wolkersdorfer C, Bowell R (2005) Contemporary reviews of mine water studies in Europe, Part 3. Mine Water Environ 24:58–76. https://doi.org/10.1007/s10230-005-0074-2
Younger PL, Wolkersdorfer C (2004) Mining impacts on the fresh water environment: technical and managerial guidelines for catchment scale management. Mine Water Environ 23:s2–s80. https://doi.org/10.1007/s10230-004-0028-0
Yuval D, Oldenburg W (1996) DC resistivity and IP methods in acid mine drainage problems: results from the Copper Clif mine waste rocks impoundments. J Appl Geophys 34:187–198. https://doi.org/10.1016/0926-9851(95)00020-8